Heliyon 6 (2020) e03560

Contents lists available at ScienceDirect

Heliyon

journal homepage: www.cell.com/heliyon

Research article

Investigation of the gamma ray shielding properties for polyvinyl chloride reinforced with chalcocite and hematite minerals

K.A. Mahmoud [a,b,*], E. Lacomme [c], M.I. Sayyed [d], Ö.F. Özpolat [e], O.L. Tashlykov [a]

[a] Ural Federal University, 19 Mira st., 620002, Yekaterinburg, Russia
[b] Nuclear Materials Authority, Maadi, Cairo, Egypt
[c] Advanced Science Research, Sophomore, Eastchester High School, Eastchester, New York, United States
[d] Physics Department, University of Tabuk, Tabuk, Saudi Arabia
[e] Computer Sciences Research and Application Center, Atatürk University, 25240 Erzurum, Turkey

ARTICLE INFO

Keywords:
Materials science
Nuclear physics
Polyvinyl chloride
Hematite
Chalcocite
Shielding parameters
Radiation shielding

ABSTRACT

Polyvinyl chloride (PVC) is the most widely produced synthetic plastic polymer in the world: it has a variety of applications due to its low cost, elasticity, light weight, good mechanical characteristics and corrosion resistance. In order to protect living beings from harmful radiation such as gamma rays, novel low-cost chalcocite and hematite-based PVCs were fabricated for shielding purposes. The mass attenuation coefficient μ_m for various fabricated hematite and chalcocite-based PVCs was calculated using MCNP-5 code. The results were compared with the values calculated theoretically using XCOM software between 0.015 and 15 MeV. Moreover, the simulated μ_m parameter for chalcocite/PVC and hematite/PVC was used to calculate other shielding factors, such as the half value layer (HVL), the mean free path (MFP) effective atomic number Z_{eff}, the geometric-progress (G-P) fitting parameters and the exposure buildup factor (EBF). The simulated data of μ_m for all composites is comparable to that obtained from a theoretical calculation. The results showed that the addition of hematite and chalcocite enhance the μ_m of PVC polymers. We also found that the μ_m of chalcocite/PVC is higher than that of hematite/PVC due to the copper content in the former.

1. Introduction

Polyvinyl chloride (PVC) is a chlorinated hydrocarbon polymer originally produced by the USA and Germany in 1930. PVC has become an important material due to its low manufacturing cost, elasticity, light weight, and corrosion resistance. It is a solid white material formed during the polymerization of polyvinyl chloride monomers with a chemical composition of $(C_2H_3Cl)_n$. The pure PVC polymers are insoluble in water, acids, and organic solvents, but they are slightly soluble in tetrahydrofuran at room temperature. Over the last few decades, PVC has become the world's mostly widely produced synthetic plastic polymer: it has a variety of applications due to its low cost, elasticity, light weight, good mechanical characteristics, and corrosion resistance [1, 2, 3].

Enhancement of the physico-mechanical properties of PVC polymers depends on the type of filler used. Numerous works have reported the enhancement effect of various filler materials on the properties of PVC. $BaTiO_3$/NiO were found to enhance the conductivity and dielectric constants of PVC [1], while $La_{0.95}Bi_{0.05}FeO_3$ nanoparticles were found to enhance the transition temperature, dielectric constant, and optical characteristics of the synthesized PVC [2]. In ZnO/PVC nanocomposite films, the glass transition temperature was found to increase with the addition of ZnO nanoparticles. This enhancement of the nanocomposite film's properties can facilitate the storage performance of a polymer battery [3]. Additionally, a few works have also reported enhancement of the strength of building materials; for example, the compressive stress of concrete can be advantageously modified by replacing some of the natural fine and coarse aggregates with PVC aggregates [4].

Today, radiation shielding is a very crucial component in radiation protection programs. It is utilized to optimize the dose of human radiation exposure in ionizing radiation practices (for example, radiation medicine, nuclear power plants, research accelerators and others). Conventionally, concrete is the most prevalent and commonly used material for radiation shielding in most facilities, such as hospitals. The cost effectiveness and vast available quantities of concrete are its main advantages as a shielding material [5, 6]. However, concrete has some disadvantages: cracks can occur after long periods of exposure to nuclear

* Corresponding author.
E-mail addresses: kmakhmud@urfu.ru, karemabdelazeem@yahoo.com (K.A. Mahmoud).

https://doi.org/10.1016/j.heliyon.2020.e03560
Received 25 July 2019; Received in revised form 4 August 2019; Accepted 4 March 2020

Table 1. Densities and chemical composition of hematite and chalcocite-based PVC.

	Chemical composition of hematite and chalcocite-based PVC (%)						
	PVC	PVC-H10	PVC-H20	PVC-H30	PVC-C10	PVC-C20	PVC-C30
SiO_2	0.000	0.093	0.186	0.279	0.009	0.018	0.027
Fe_2O_3	0.000	0.000	0.000	0.000	0.000	0.000	0.000
Al_2O_3	0.000	0.016	0.032	0.048	0.000	0.000	0.000
CaO	0.000	0.009	0.018	0.027	0.000	0.000	0.000
MgO	0.000	0.101	0.202	0.303	0.000	0.000	0.000
C_2H_3Cl	99.900	89.910	79.920	69.930	89.910	79.920	69.930
TiO_2	0.000	0.004	0.008	0.012	0.000	0.000	0.000
FeO	0.000	8.853	17.706	26.559	0.014	0.028	0.042
Cu	0.000	0.000	0.000	0.000	7.967	15.934	23.901
S	0.000	0.000	0.000	0.000	2.016	4.032	6.048
Density (g/cm^3)	1.192	1.649	2.102	2.551	1.830	2.467	3.105

radiation and it is difficult to transport. Synthetic polymers can be utilized to fabricate new materials that can provide radiation shielding. Moreover, their other advantages (low manufacturing cost, durability, and high thermal and chemical stability) are among the favored traits and qualities for superior shielding materials. Recently, many works have reported various kinds of polymers, such as nylon-6, have novel shielding properties and can be used for protection against neutrons [7]. Moreover, other works have noted the effects of various fillers on the neutron shielding properties of polymers; for instance, the shielding properties of siloxane-based polymers were enhanced by the addition of boron particles [8]. Furthermore, the efficiency of epoxy resin was improved with molybdenum [9], barite [10] and a ferrochromium slag additive [11].

Hematite and chalcocite are two minerals rich in iron and copper, respectively. They are natural, cheap, abundant, and have suitable mass attenuation coefficients for low and high gamma rays [12]. In the present work, PVCs were synthesized and fabricated with chalcocite and hematite. The mass attenuation coefficient μ_m for five various polymer samples was calculated using MCNP-5 Code between 0.015 and 15 MeV. Gamma ray interaction and penetration were evaluated by calculating other shielding parameters such as the half value layer (HVL), the effective atomic number Z_{eff}, the effective electron density N_{el} and the exposure buildup factor (EBF). In order to test the reliability of the results obtained from the MCNP simulation, the μm obtained by MCNP simulation code were compared to those calculated theoretically using the XCOM database.

2. Materials and methods

2.1. Theoretical aspect

Shielding materials can be characterized through their mass attenuation coefficient μm. The theoretical calculation of μm for PVC, PVC/hematite and PVC/chalcocite can be reached via Eq. (1) [13]:

$$\mu_m\left(\frac{cm^2}{g}\right) = \sum_{i=0}^{n} \omega_i \left(\frac{\mu}{\rho}\right)_i \quad (1)$$

Where ωi and $\left(\frac{\mu}{\rho}\right)_i$ are the fractional weight and partial mass attenuation coefficients, respectively, for the i^{th} constituent element in multielement modified materials.

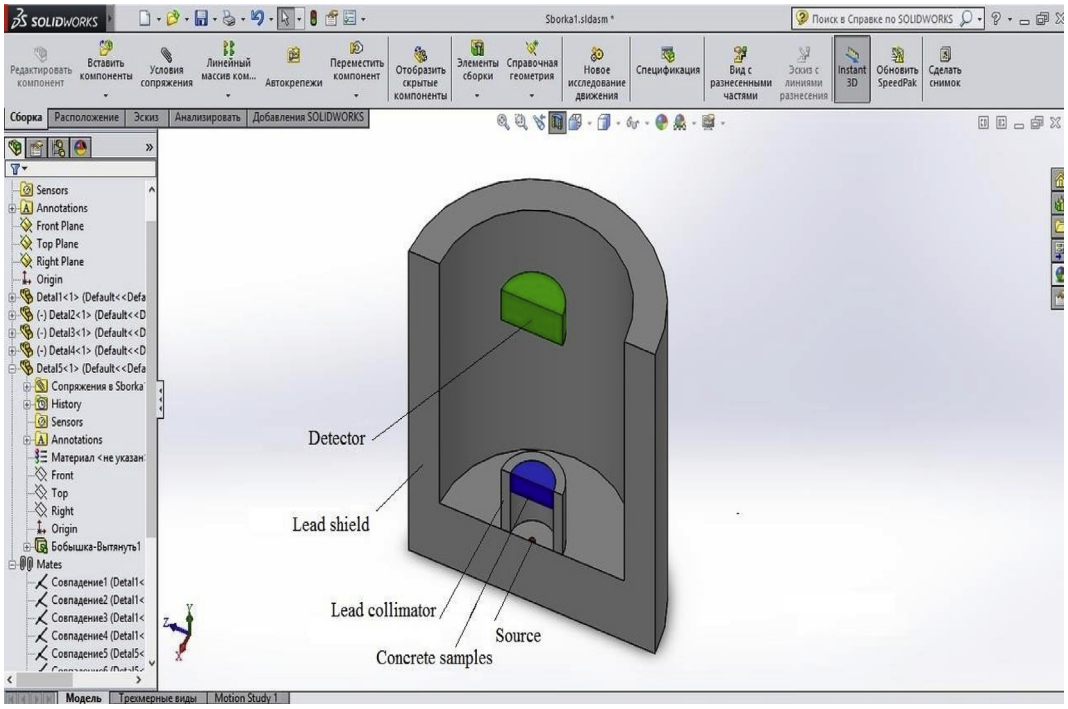

Figure 1. Screen shot for MCNP geometry.

The mean free path (MFP) is the shielding parameter which describes the distance that gamma ray photons travel inside the shielding material between two successive collisions. The half value layer (HVL) is the thickness required to decrease gamma ray intensity to half of its initial value (HVL). The MFP and HVL can be described by Eqs. (2) and (3):

$$MFP\ (cm) = \frac{1}{\mu\ (cm^{-1})} \tag{2}$$

$$HVL\ (cm) = \frac{0,693}{\mu\ (cm^{-1})} \tag{3}$$

The effective atomic number Z_{eff} is an important factor in shielding materials: it describes any multi-element shielding material in terms of its equivalent element and is defined through the following equation [14]:

$$Z_{eff} = \frac{\sum_i f_i A_i (\mu_m)_i}{\sum_j \frac{A_i}{Z_j} (\mu_m)_j} \tag{4}$$

Where f_i, A_i and Z_j refer to the fractional abundance, atomic weight and atomic number of the i^{th} constituent element, respectively.

Effective electron density N_{eff} is also a factor in radiation shielding and is defined through Eq. (5):

$$N_{eff} = \frac{N_A}{M} Z_{eff} \sum n_i \tag{5}$$

Where M is the atomic mass of the material.

2.2. PVC preparation

Hematite and chalcocite-based PVC mixtures were fabricated to produce a new material that possesses superiority shielding properties. A commercial-grade PVC was melted at a temperature of 250 °C and then reinforced with multiple ratio contents of hematite and chalcocite minerals. The mixtures were prepared in 2 different types of polymer for different fillers of hematite and chalcocite. They were labeled as PVC- H10, PVC- H20, and PVC-H30 for hematite ratios of 10, 20, and 30%, respectively, while the other series was labeled as PVC-C10, PVC-C20, and PVC-C30 for chalcocite ratios of 10, 20, and 30%, respectively. The ratio of hematite and chalcocite cannot exceed 30% if the elasticity of the PVC composites is to be maintained.

X-ray fluorescence (XRF) was used to determine the chemical composition of the fabricated samples while the density of the fabricated samples was measured using the Archimedes method. The compositions and densities are listed in Table 1.

MCNP is a radiation transport code developed by created by the Los Alamos National Laboratory (LANL). It is used to simulate the transport of electrons, neutrons, gamma, and X-rays using the Monte Carlo method [15]. The MCNP input file required accurate information about the geometry, source (SDEF card), and composition (material card) to execute a MCNP simulation. The geometry of the simulation was designed according to an arbitrary 3D setup, as illustrated in Figure 1. As shown in Figure 1, all equipment has been considered according to experimental facilities. The radioactive source was placed inside a lead collimator with a slit diameter of 2 cm. The source was placed at a distance of 10 cm from the detector. The samples were fabricated as a disk with a diameter of 5 cm placed between the source and the detector at a distance of 5 cm from the source. The detector was set up to be an F2 tally in order estimate the track length of the incident gamma ray. The simulation geometry shielded the outer space using 5cm of lead. The simulation was carried out using NPS card = 10^6 particles. The relative error estimated from the MCNP simulation is less than 1%.

3. Results and discussion

The simulations of the irradiation of the PVC, PVC/hematite, and PVC/chalcocite samples were carried out using MCNP radiation transport code and monoenergetic photon sources of 0.015 and 15 MeV to calculate the μ_m of the samples. Figure 2 illustrates that the μ_m for all the samples tends to peak at values of lower energy (i.e. 0.015 MeV) due to the photoelectric cross section, which is largely present in the low energy region. According to Table 2, the maximum μ_m of all composites varied between 10.456 and 25.974 cm^2/g for PVC and PVC-C30 composites, respectively. The variation of the maximum μ_m reveals the dependence of μ_m on the composition of the materials.

Figure 2 also reveals that the μ_m in intermediate energy (i.e. $0.06 < E < 2$ MeV) has low variation with the incident gamma ray energy due to the Compton scattering that dominates in this energy interval. In addition, the μ_m of all the composites is almost constant for high energies (i.e. $E > 3$ MeV) due to the pair production interaction in which the interaction cross section mainly depends on the energy of the incident gamma ray. It is clear from Figure 2 that the simulated μ_m of the PVC polymer is enhanced due to the addition of chalcocite and hematite minerals.

It can also be seen that the μ_m of chalcocite/PVC is higher than that of hematite/PVC due to the copper content in the former, which has a higher μ_m than the iron content in hematite/PVC. The simulated μm of the prepared PVC, PVC/hematite, and PVC/chalcocite compared with some commercial shielding materials such as ordinary concrete [16], zinc bismuth borate glass ($10ZnO; 30Bi_2O_3;60B_2O_3$) [17], and RS-520(SF6) glass [18]. The comparison showed that our studied samples have a μ_m higher than concrete, while they have μm lower than zinc bismuth borate glass and RS-520 glass (at low and intermediate energy). At high gamma ray energy ($E > 3$ MeV), the μ_m for all studied samples and standard shielding materials are comparable. The theoretical μ_m was computed using the XCOM database. The simulated results of the μ_m for PVC, PVC/hematite, and PVC/chalcocite were comparable to those calculated using XCOM, which indicates the reliability of the values for the μ_m showed in Table 2. The difference in percentage between the simulated and calculated μ_m for all composites was found to be less than 1%.

Better shielding materials show thinner layers of HVL and MFP [19]. The energy dependence of MFP for hematite/PVC and chalcocite/PVC is illustrated in Figure 3. It is clear that the MFP of all composites tends to peak at high energies (i.e. 15 MeV) and varies between 13.101 and 38.357 cm for PVC and PVC-C30 respectively, while the MFP tends to be

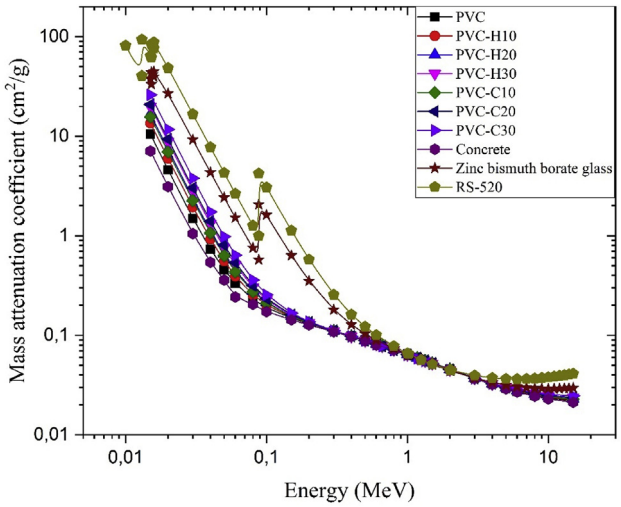

Figure 2. The Mass attenuation coefficient of hematite-based PVC, chalcocite-based PVC and other commercial shielding materials.

Table 2. Comparison between simulated and calculated μm.

Energy (MeV)	Mass attenuation coefficient (cm^2/g)													
	PVC		PVC-H10		PVC-H20		PVC-H30		PVC-C10		PVC-C20		PVC-C30	
	MCNP	XCOM	MCNP	XCOM	MCNP	XCOM	MCNP	XCOM	MCNP	XCOM	MCNP	XCOM	MCNP	XCOM
0.015	10.456	10.450	13.5137	13.4100	16.6528	16.6300	19.7812	19.8100	15.6302	15.6200	20.7883	20.8200	25.9748	25.9800
0.02	4.582	4.579	5.9711	5.9210	7.3964	7.3820	8.8168	8.8240	6.9559	6.9500	9.3220	9.3360	11.7015	11.7000
0.03	1.492	1.492	1.9338	1.9180	2.3869	2.3830	2.8383	2.8410	2.2568	2.2550	3.0189	3.0230	3.7851	3.7840
0.04	0.731	0.730	0.9225	0.9152	1.1195	1.1170	1.3156	1.3160	1.0659	1.0640	1.4001	1.4010	1.7360	1.7340
0.05	0.456	0.456	0.5556	0.5518	0.6578	0.6563	0.7594	0.7593	0.6311	0.6304	0.8056	0.8059	0.9808	0.9799
0.06	0.333	0.332	0.3903	0.3882	0.4496	0.4488	0.5086	0.5087	0.4346	0.4343	0.5365	0.5368	0.6388	0.6384
0.08	0.230	0.230	0.2539	0.2531	0.2788	0.2784	0.3035	0.3034	0.2730	0.2728	0.3161	0.3162	0.3593	0.3591
0.1	0.189	0.189	0.2008	0.2003	0.2132	0.2130	0.2255	0.2254	0.2105	0.2105	0.2324	0.2324	0.2542	0.2541
0.15	0.148	0.149	0.1515	0.1515	0.1547	0.1547	0.1578	0.1579	0.1543	0.1544	0.1603	0.1603	0.1661	0.1662
0.2	0.131	0.131	0.1316	0.1317	0.1326	0.1326	0.1335	0.1336	0.1327	0.1328	0.1348	0.1348	0.1368	0.1368
0.3	0.111	0.111	0.1106	0.1108	0.1106	0.1106	0.1104	0.1105	0.1108	0.1110	0.1110	0.1111	0.1110	0.1111
0.4	0.099	0.099	0.0982	0.0983	0.0978	0.0979	0.0974	0.0975	0.0981	0.0983	0.0978	0.0979	0.0974	0.0975
0.5	0.090	0.090	0.0892	0.0894	0.0888	0.0889	0.0884	0.0884	0.0891	0.0893	0.0887	0.0887	0.0881	0.0882
0.6	0.083	0.083	0.0823	0.0825	0.0819	0.0820	0.0814	0.0815	0.0822	0.0824	0.0817	0.0818	0.0811	0.0812
0.662	0.079	0.079	0.0787	0.0789	0.0783	0.0784	0.0779	0.0780	0.0786	0.0788	0.0781	0.0782	0.0775	0.0776
0.8	0.073	0.073	0.0722	0.0723	0.0718	0.0718	0.0713	0.0714	0.0720	0.0722	0.0715	0.0716	0.0709	0.0710
1	0.065	0.065	0.0646	0.0649	0.0643	0.0645	0.0638	0.0641	0.0645	0.0648	0.0640	0.0643	0.0634	0.0637
1.173	0.060	0.060	0.0597	0.0600	0.0593	0.0596	0.0589	0.0592	0.0595	0.0598	0.0591	0.0593	0.0585	0.0588
1.332	0.056	0.057	0.0559	0.0562	0.0556	0.0558	0.0552	0.0554	0.0558	0,0561	0,0554	0,0556	0,0549	0,0551
1.5	0.053	0.053	0.0527	0.0529	0.0523	0.0525	0.0520	0.0522	0.0525	0.0528	0.0521	0.0523	0.0517	0.0519
2	0.046	0.046	0.0455	0.0456	0.0452	0.0454	0.0450	0.0451	0.0454	0.0455	0.0451	0.0452	0.0448	0.0449
3	0.037	0.037	0.0371	0.0373	0.0370	0.0372	0.0369	0.0370	0.0371	0.0373	0.0370	0.0372	0.0369	0.0370
4	0.033	0.033	0.0325	0.0326	0.0325	0.0326	0.0325	0.0326	0.0326	0.0327	0.0326	0.0327	0.0327	0.0328
5	0.030	0.030	0.0296	0.0297	0.0297	0.0298	0.0298	0.0299	0.0297	0.0298	0.0299	0.0300	0.0301	0.0302
6	0.027	0.028	0.0276	0.0277	0.0278	0.0279	0.0280	0.0281	0.0278	0.0278	0.0281	0.0282	0.0284	0.0285
8	0.025	0.025	0.0252	0.0253	0.0255	0.0256	0.0258	0.0259	0.0254	0.0255	0.0259	0.0260	0.0264	0.0265
10	0.024	0.024	0.0239	0.0239	0.0243	0.0244	0.0247	0.0248	0.0241	0.0242	0.0248	0.0249	0.0254	0.0255
15	0.022	0.022	0.0224	0.0225	0.0230	0.0230	0.0236	0.0236	0.0228	0.0228	0.0237	0.0237	0.0246	0.0246

at its lowest for all composites at low energies (i.e. 0.015 MeV) and varies between 0.0123 cm and 0.0802 cm for PVC- C30 and PVC respectively. In the low energy region ($0.015 < E < 0.06$ MeV), the MFP tends to be at its lowest for all composites and also varies slightly with the incident energy due to the photoelectric interaction in which the interaction cross section is mainly proportional to Z^{4-5} [20, 21, 22]. The MFP increases gradually for all composites with the increase of the incident gamma ray energy (for $0.06 < E < 3$ MeV) due to the Compton effect in which the interaction cross section is directly proportional to the incident gamma ray energy. Finally, at the high energy region (for $E > 3$ MeV) in which the pair production interaction domains, the MFP increases rapidly with the energy increase. According to the previous discussion the sample

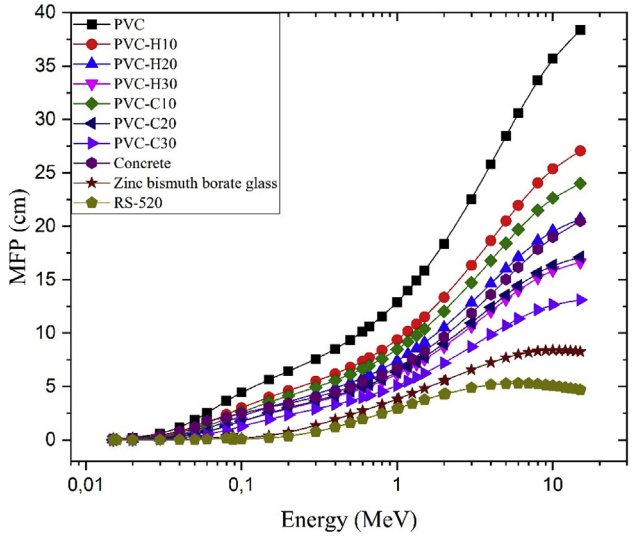

Figure 3. Comparison between the MFP of PVC/Hematite, PVC/Chalcocite and some commercial shielding materials.

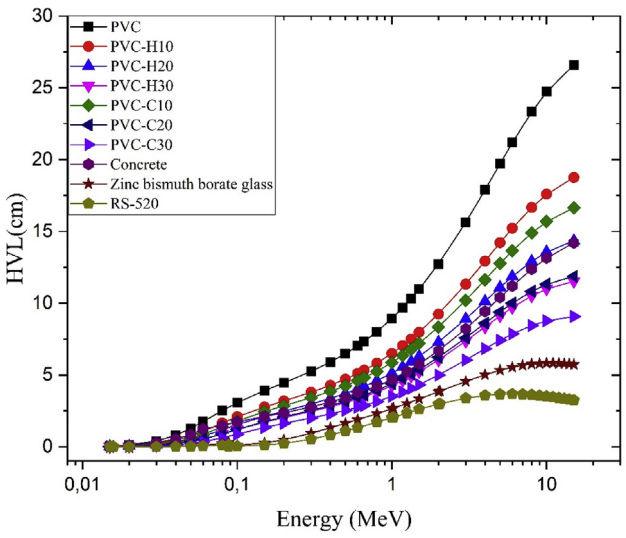

Figure 4. Th variation of HVL with energy for hematite-based PVC, chalcocite-based PVC and other commercial shielding materials.

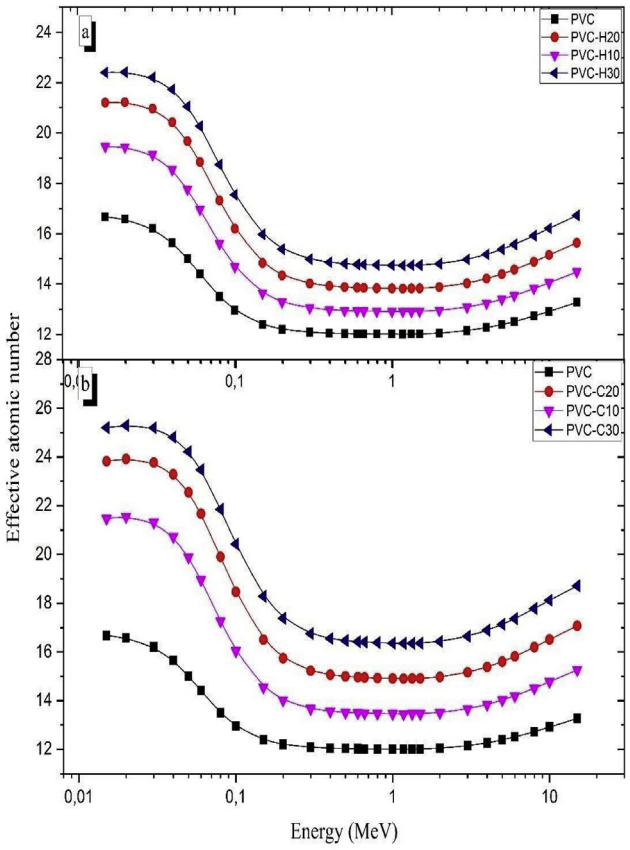

Figure 5. The effective atomic number for (a) hematite-based PVC and (b) chalcocite-based PVC.

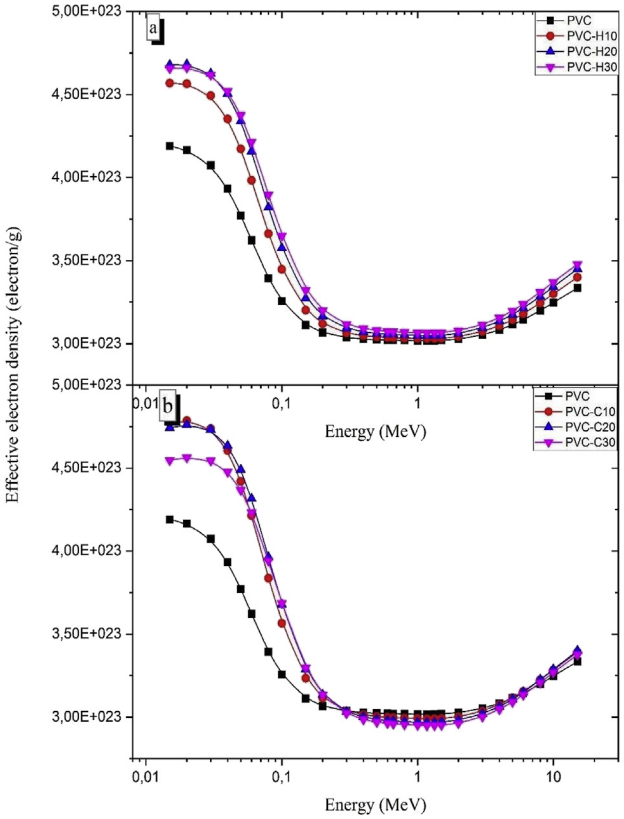

Figure 6. The variation of composites effective electron density with the incident energy (a) hematite-based PVC and (b) chalcocite-based PVC.

PVC-C30 is considered the most effective shielding material in our study due to its low MFP. The MFP of PVC-C30 varied between 0.0123 and 13.101 cm and found to be lower than the ordinary concrete which varied between 0.0614 and 20.489 cm between 0.015 and 15 MeV respectively. The MFP of PVC-C30 found to be higher than the heavy metal oxides and glass which varied between 0.006-8.262 cm and 0.003–4.687 cm respectively.

The mechanism in which the HVL varied with the incident gamma ray energy is illustrated in Figure 4. Figure 4 reveals that the HVL values for all the prepared composites can be described in the similar manner as the MFP. However, the maximum HVL varied between 9.080 and 26.599 cm for PVC- C30 and PVC respectively, and the lowest HVL varied between 0.008 and 0.055 cm for the same composites. The HVL of PVC-C30 found to be lower than the HVL of ordinary concrete which varied between 0.0425 and 14.199 cm while, it is higher than the HVL of heavy metal oxides and glass RS-520 which varied between 0.004-5.726cm and 0.002–3.248 cm respectively.

Effective atomic number Z_{eff} is required to describe the shielding parameters of a multi-element composite as its equivalent element. The energy dependence of the Z_{eff} is illustrated in Figure 5 (a and b). The Z_{eff} tends to peak at values for composites of low energy (for $E = 0.015$ MeV) because of the dominance of the photoelectric effect, and varies between 16.67 and 25.2 for PVC and PVC-C30 respectively. On the other hand, the minimum values were found at intermediate energies ($0.2 < E < 3$ MeV) and varied between 12.01 and 16.34 for PVC and PVC-C30 respectively. In addition, it can be observed that the Z_{eff} is nearly constant for all composites in the intermediate energy region ($0.2 < E < 3$ MeV) due to the Compton effect. The z_{eff} increased slowly with the increase of the incident gamma ray energy ($E > 3$ MeV) due to the pair production interaction in which the cross section in directly proportional to (log E) [23, 24, 25].

It can also observe that the Zeff for PVC increased with the addition of hematite and chalcocite, while chalcocite/PVC have higher Z_{eff} than PVC and hematite/PVC composites due to the copper contents, which have a high efficiency in gamma ray shielding.

The energy dependence of the effective electron density N_{eff} is shown in Figure 6 (a and b), which reveals that the variation of N_{eff} with the incident gamma ray energy is similar to the variation of Z_{eff}, and as a result, it can be described in a similar manner. The highest N_{eff} was obtained in the energy value of 0.015 MeV and varied between 4.19×10^{23} and 4.77×10^{23} (electron/g) for PVC and PVC-H10 respectively, while

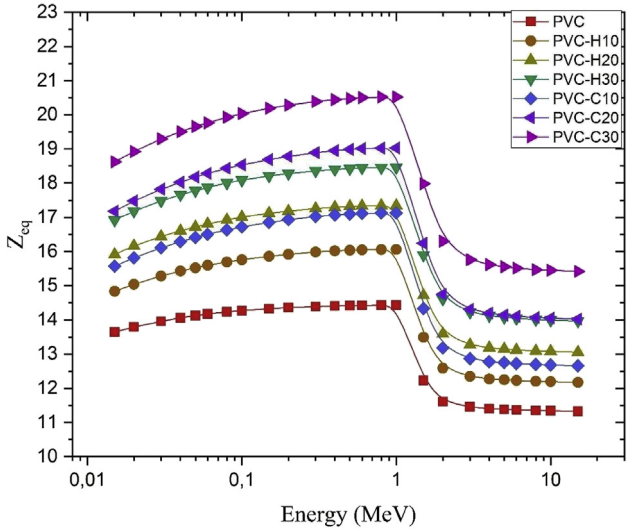

Figure 7. The variation of the Z_{eq} of PVC, hematite/PVC and chalcocite/PVC with the incident gamma ray energy.

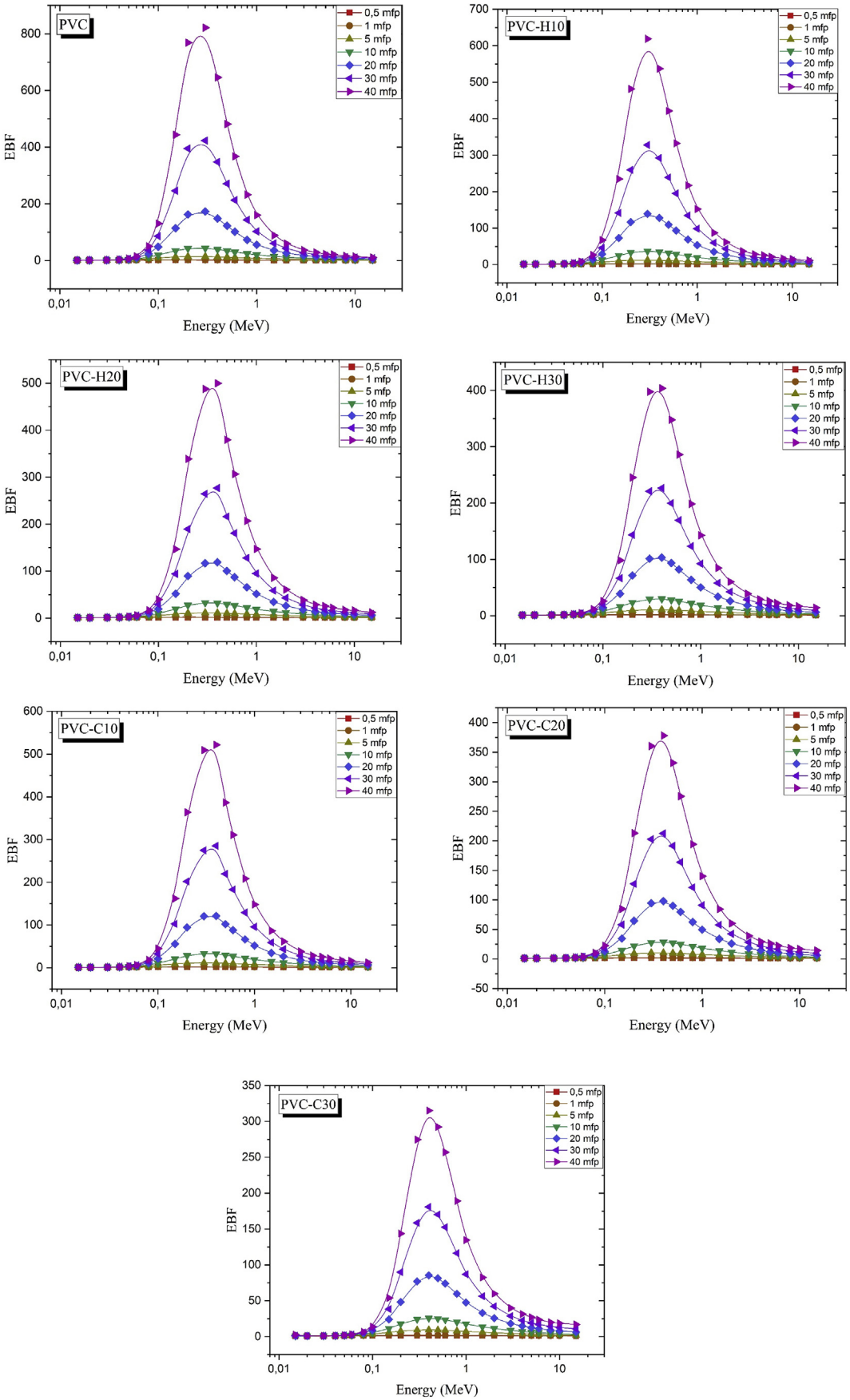

Figure 8. The variation of EBF with gamma ray energy for PVC, hematite/PVC and chalcocite/PVC composites.

the lowest N_{eff} was achieved at energy of 1.332 MeV and varied between 2.95×10^{23} and 3.07×10^{23} (electron/g) for PVC-C30 and PVC- H10. Furthermore, it can be observed that in the intermediate energy region ($0.3 < E < 3$ MeV) the addition of hematite increases the N_{eff} of the PVC, while the addition of chalcocite decreases the N_{eff} of the PVC.

The best shielding material is that which have high equivalent atomic number. The equivalent atomic number Z_{eq} for PVC, hematite/PVC and chalcocite/PVC was calculated between 0.015 and 15 MeV and illustrated in Figure 7. It is clear that for all composites the Z_{eq} tends to maximum values varied between 14.43 and 20.52 for PVC and PVC-C30 respectively at energy between 0.8 and 1 MeV while, it tends to minimum values at high energy. For gamma ray energy between 0.015 and 1 MeV there are a small variation of Z_{eq} with the incident energy due to Compton scattering which is domains in the intermediate gamma ray energy. In the other hand, the Z_{eq} is rapidly decrease for energy $E > 1$ MeV due to the pair production interaction. Furthermore, the G-P fitting parameters for PVC, hematite/PVC and chalcocite/PVC were calculated and listed in supplementary data Table S1.

The exposure buildup factor EBF of various prepared PVC composites calculated using geometric-progress fitting parameters (G-P fitting parameters) between 0.015 and 15 MeV and presented in Figure 8. It is clear that, EBF tends to maximum for all composite's values at penetrating depth 40 mfp while, it tends to minimum values at penetrating depth 0.5 mfp. Moreover, the EBF of PVC, hematite/PVC and chalcocite/PVC increase with increasing the penetration depth. The highest EBF for all concretes is achieved in the intermediate energy (i.e. $0.3 < E < 0.5$ MeV) due to the Compton scattering domination. The highest value of the EBF is obtained for PVC composites and varied between 1.6 and 822 at 0.5 and 40 mfp respectively, while the lowest EBF is obtained for PVC-C30 and varied between 1.54 and 315 at 0.5 and 40 mfp respectively. Figure 8 reveals to the additive of chalcocite and hematite decrease the EBF.

4. Conclusion

The shielding parameters of PVC, hematite/PVC and chalcocite/PVC composites are studied between ($0.015 < E < 15$ MeV) using MCNP code. The simulated results of μ_m for all composites showed their dependence on the incident gamma ray energy. The highest μ_m obtained for PVC-C30 composite and varied between 25.98 and 0.024 cm^2/g, while the lowest μ_m obtained for the PVC has values between 10.456 and 0.022 cm^2/g and varied between 0.015 and 15 MeV respectively. The shielding parameters of the fabricated PVC compared to some commercial shielding materials. The comparison showed that the shielding parameters of PVC materials are better than those of ordinary concrete while, they are less than the shielding parameters of zinc bismuth borate glass and RS-520 glass. Furthermore, the simulated data of μ_m are close to those calculated using XCOM for all composites. The study showed that the addition of hematite and chalcocite enhance the mass attenuation coefficient of PVC polymers. But chalcocite/PVC have a higher mass attenuation coefficient than hematite/PVC composites. Moreover, the results showed that a thin layer of chalcocite/PVC composite was sufficient to shield the incident gamma ray at various energies, compared to hematite/PVC. The obtained results showed that chalcocite/PVC and hematite/PVC composites have adequate shielding properties and they will be useful in various shielding applications.

Declarations

Author contribution statement

K. A. Mahmoud: Conceived and designed the experiments; Performed the experiments; Analyzed and interpreted the data; Wrote the paper.

E. Lacomme: Analyzed and interpreted the data; Wrote the paper.

M. I. Sayyed: Conceived and designed the experiments; Analyzed and interpreted the data; Contributed reagents, materials, analysis tools or data; Wrote the paper.

Ö. F. Özpolat: Performed the experiments; Analyzed and interpreted the data; Contributed reagents, materials, analysis tools or data.

O. L. Tashlykov: Conceived and designed the experiments; Performed the experiments; Contributed reagents, materials, analysis tools or data.

Funding statement

This research did not receive any specific grant from funding agencies in the public, commercial, or not-for-profit sectors.

Competing interest statement

The authors declare no conflict of interest.

Additional information

Supplementary content related to this article has been published online at https://doi.org/10.1016/j.heliyon.2020.e03560.

References

[1] A. Muzaffar, M.B. Ahamed, K. Deshmukh, M. Faisal, Electromagnetic interference shielding properties of polyvinylchloride (PVC), barium titanate (BaTiO3) and nickel oxide (NiO) based nanocomposites, Polym. Test. (2019).
[2] T.A. Taha, A.A. Azab, nanocomposites, J. Mol. Struct. 1178 (2019) 39–44.
[3] I.S. Elashmawi, N.A. Hakeem, L.K. Marei, F.F. Hanna, Structure and performance of ZnO/PVC nanocomposites, Phys. B Phys. Condens. Matter. 405 (2010) 4163–4169.
[4] A.A. Mohammed, I.I. Mohammed, S.A. Mohammed, Some properties of concrete with plastic aggregate derived from shredded PVC sheets, Construct. Build. Mater. 201 (2019) 232–245.
[5] K.A. Mahmoud, O.L. Tashlykov, A.F. El Wakil, I.E. El Aassy, Aggregates grain size and press rate dependence of the shielding parameters for some concretes, Prog. Nucl. Energy 118 (2020) 103092.
[6] A.M. Abu El-soad, M.I. Sayyed, K.A. Mahmoud, E. Şakar, E.G. Kovaleva, Simulation studies for gamma ray shielding properties of Halloysite nanotubes using MCNP-5 code, Appl. Radiat. Isot. (2019) 108882.
[7] M.R. Kaçal, F. Akman, M.I. Sayyed, Evaluation of gamma-ray and neutron attenuation properties of some polymers, Nucl. Eng. Technol. 51 (2019) 818–824.
[8] A. Labouriau, T. Robison, C. Shonrock, S. Simmonds, B. Cox, A. Pacheco, C. Cady, Boron filled siloxane polymers for radiation shielding, Radiat. Phys. Chem. 144 (2018) 288–294.
[9] B. Aygün, T. Korkut, A. Karabulut, O. Gencel, A. Karabulut, Production and neutron irradiation tests on a new epoxy/molybdenum composite, Int. J. Polym. Anal. Char. 20 (2015) 323–329.
[10] M.A. El-Sarraf, A. El-Sayed Abdo, Insulating epoxy/barite and polyester/barite composites for radiation attenuation, Appl. Radiat. Isot. 79 (2013) 18–24.
[11] T. Korkut, O. Gencel, E. Kam, W. Brostow, International Journal of Polymer Analysis and Characterization X-Ray , Gamma , and Neutron Radiation Tests on Epoxy-Ferrochromium Slag Composites by Experiments and Monte Carlo Simulations, 2013, pp. 37–41.
[12] K.A. Mahmoud, M.I. Sayyed, O.L. Tashlykov, Comparative studies between the shielding parameters of concretes with different additive aggregates using MCNP-5 simulation code, Radiat. Phys. Chem. (2019) 108426.
[13] F. Akman, M.R. Kaçal, M.I. Sayyed, H.A. Karataş, Study of gamma radiation attenuation properties of some selected ternary alloys, J. Alloys Compd. 782 (2019) 315–322.
[14] B. Oto, N. Yildiz, F. Akdemir, E. Kavaz, Investigation of gamma radiation shielding properties of various ores, Prog. Nucl. Energy 85 (2015) 391–403.
[15] J. Briesmeister, MCNP – a General Monte Carlo Code for Neutron and Photon Transport, National Laboratory, Los Alamos, 2000. Report LA13709-M, version 4C.
[16] I.I. Bashter, A.S. Makarious, E.S. Abdo, Investigation of hematite-serpentine and ilmenite-limonite concretes for reactor radiation shielding, Ann. Nucl. Energy 23 (1996) 65–71.
[17] P. Yasaka, N. Pattanaboonmee, H.J. Kim, P. Limkitjaroenporn, J. Kaewkhao, Gamma radiation shielding and optical properties measurements of zinc bismuth borate glasses, Ann. Nucl. Energy 68 (2014) 4–9.
[18] A.G. Schoot, Radiation shielding glasses. http://www.schott.com/advanced_optics/english/products/optical- materials/special materials/radiation-shielding-glasses/index.html.
[19] M.I. Sayyed, F. Akman, A. Kumar, M.R. Kaçal, Evaluation of radioprotection properties of some selected ceramic samples, Results Phys. 11 (2018) 1100–1104.
[20] M.G. Dong, M.I. Sayyed, G. Lakshminarayana, M. Çelikbilek Ersundu, A.E. Ersundu, P. Nayar, M.A. Mahdi, Investigation of gamma radiation shielding properties of

lithium zinc bismuth borate glasses using XCOM program and MCNP5 code, J. Non-Cryst. Solids 468 (2017) 12–16.
[21] M.I. Sayyed, M.G. Dong, H.O. Tekin, G. Lakshminarayana, M.A. Mahdi, Comparative investigations of gamma and neutron radiation shielding parameters for different borate and tellurite glass systems using WinXCom program and MCNPX code, Mater. Chem. Phys. 215 (2018) 183–202.
[22] Sazirul Islam, K.A. Mahmoud, M.I. Sayyed, Bünyamin Alim, Md M. Rahman, A.S. Mollah, Study on the radiation attenuation properties of locally available beeswax as a tissue equivalent bolus material in radiotherapy, Radiat. Isot. (2019) 108559.
[23] U. Kaur, J.K. Sharma, P.S. Singh, T. Singh, Comparative studies of different concretes on the basis of some photon interaction parameters, Appl. Radiat. Isot. 70 (2012) 233–240.
[24] K.A. Mahmoud, M.I. Sayyed, O.L. Tashlykov, Gamma ray shielding characteristics and exposure buildup factor for some natural rocks using MCNP- 5 code, Nucl. Eng. Technol. 51 (2019) 1835–1841.
[25] K.A. Mahmoud, Y.S. Rammah, Investigation of gamma-ray shielding capability of glasses doped with Y, Gd, Nd, Pr and Dy rare earth using MCNP-5 code, Phys. B Phys. Condens. Matter (2020) 411756.